Printed ISSN 1330–0008
Online ISSN 1333–9125
CD ISSN 1333–8390
CODEN FIZAE4

STUDY OF VELOCITY-DEPENDENT COLLISION EFFECTS ON LAMB DIP AND CROSSOVER RESONANCES IN THREE-LEVEL SYSTEM

BIBHAS K. DUTTA[a] and PRASANTA K. MAHAPATRA[b]

[a]*Department of Physics, J. K. College, Purulia – 723 101, India*

[b]*Department of Physics and Technophysics, Vidyasagar University, Midnapore – 721 102, India*

Received 20 September 2005; Accepted 13 December 2006
Online 23 February 2007

We discuss the effects of phase-dephasing and velocity-changing collisions on saturated absorption line shapes studied in an open V-type system under the semiclassical density-matrix formalism. It has been noted that the traces of Lamb dips and crossover resonance dip lying within the Doppler-broadened contour can vanish in the presence of a strong saturating field if a sufficient contribution of collisional dephasing effect is present. Asymmetry may be introduced in the wings of saturated line profiles for a small contribution of collision kernel.

PACS numbers: 32.70.Jz, 33.70.-w, 33.70.Jg UDC 539.186

Keywords: three level systems, saturation spectroscopy, Lamb dip and crossover resonances, phase-dephasing and velocity-changing collisions

1. Introduction

When exposed to a sufficiently strong external field, multilevel atomic systems exhibit nonlinear effects. The most fundamental nonlinear spectroscopic effect is known as the laser saturation process that renders the elimination of inhomogeneous broadening effect in spectral profile due to spectral hole burning (SHB) [1, 2]. The phenomenon occurs when there is an appreciable reduction of absorption of a coherent field (called the probe field) tuned at resonance, with a transition that is simultaneously viewed by another coherent field (called the saturating or the pump field) propagating in opposite direction of the first one. More physically, the probe field encounters a hole created by the pump in the population distribution curve of the lower resonant level. This leads to Doppler-free Lorentzian profile called the Lamb dip [3] within the Doppler-broadened absorption line shape

obtained on probe detuning. The width of the Lamb dip is basically controlled by the natural decay rates related to the resonant levels and the saturation broadening caused by the strong applied field. In collision-induced media, the collisional relaxation may substantially affect the generation of Lamb dip within the Doppler-broadened contour. Haroche and Hartmann [4] studied the saturated absorption line shape for a two-level atomic system irradiated by a weak probe and strong pump fields in counter-propagating configuration. In a theoretical analysis of the saturated Doppler-broadened resonances involving two closely spaced upper levels and a single lower level, Schlossberg and Javan [5] reported that in spite of the Lamb dips, an additional dip could be found exactly halfway between two Lamb dips for a smaller energy difference between the upper levels than the corresponding Doppler widths. The additional dip is known as the crossover-resonance dip, that appears beacuse the hole burnt by the pump field in one transition is monitored by the probe field for the other transition sharing the same lower level. Such additional dips were experimentally observed in the laser saturation spectroscopy [6] of Balmer H_α line of hydrogen and also in the infrared Zeeman spectra of methane by laser saturated absorption technique [7]. In recent years, there has been a considerable interest for the high-resolution study of hyperfine spectral lines of atomic vapours [8 – 12]. The method of Lamb dip spectroscopy finds its present-day application in the frequency locking of diode laser by optical feedback from an external cavity containing a cell of atomic vapour at ambient temperature conditions [13]. In high-resolution saturation-spectroscopic study of D_1 and D_2 lines of Na at collision environment, Hansch et al. [14] predicted a finite effect of collisional diffusion in velocity space to the line shape of Lamb dip. The combined effect of the phase-dephasing collision (PDC) and the velocity-changing collision (VCC) may be significant in modification of saturation behaviour of the Doppler-free resonances. In order to describe the collision effects in gas lasers, a theoretical study incorporating PDC and VCC into saturated population difference of two level atom has been made in Ref. [15]. Sing and Agarwal [16] investigated the effects of saturation and VCC on nearly degenerate four-wave mixing (FWM) signal in a two-level system. In this paper, we are interested to study the effects of PDC and VCC into saturated absorption-line shape for the V-type system which was similarly taken in earlier works [5, 17]. We have noticed that the formation of Lamb dip can be sustained up to a certain limit of collisional perturbation. An attempt has been made to exhibit the asymmetry induced by VCC in the wings of Doppler-free profiles within Doppler-broadened background.

2. *Theoretical formulation*

We consider an open V-type atomic system with a nondegenarate ground level $|1\rangle$ and two successive upper levels $|2\rangle$ and $|3\rangle$. The transitions $|1\rangle \leftrightarrow |2\rangle$ and $|1\rangle \leftrightarrow |3\rangle$ are specified by the frequencies ω_{12} and ω_{13}, respectively. ω_{23} is taken to be the frequency separation between the two closely-spaced upper levels $|3\rangle$ and $|2\rangle$. The rates at which the atoms are injected to the energy levels from outside the three-level atom subspace are denoted as Λ_m $(m = 1, 2, 3)$. The system is supposed

to be interacted by a standing wave formed by two counter-propagating coherent fields along the z-direction. The expression for the standing wave field can be given as $E(z,t) = \epsilon \cos\omega t \sin k_z z$; ϵ is the field amplitude, ω is the frequency of radiation field and k_z is the propagation vector. The Hamiltonian of the system can be given as $H = H_0 - \mu_{1j}E(z,t)$; $j = 2,3$ and H_0 is the unperturbed Hamiltonian. The coupling between atom and standing wave is characterized by the Rabi frequencies, $R_{1j} = \mu_{1j}\epsilon/\hbar$ and the detuning parameters, $\Delta_{1j} = \omega_{1j} - \omega$. The response of the atom moving with velocity v along the z-direction to the standing wave can be illustrated by the semiclassical density-matrix equation of the following form,

$$\left(\frac{\partial}{\partial t} + v\frac{\partial}{\partial z}\right)\rho' = -\frac{\mathrm{i}}{\hbar}\big[H,\rho'\big] + \Upsilon - \mathcal{L}\rho' + \left(\frac{\partial\rho'}{\partial t}\right)_{\text{collision}}, \tag{1}$$

where the excitation matrix, $\Upsilon_{mn} = \Lambda_m\delta_{mn}$ $(m,n = 1,2,3)$, initiates the level population consistent with the equilibrium and the relaxation operator, $\mathcal{L}_{mn} = \gamma_m\delta_{mn}$, and includes the contributions of the spontaneous decay from the energy levels. Here γ_m are the longitudinal decay rates of the respective levels. The transverse decay rates can be expressed as $\gamma_{1j} = (\gamma_1 + \gamma_j)/2$ [18]. The Raman coherence decay rate, γ_{23} is taken as the unit for all decay rates presented in the paper. In our model, we consider the phenomena PDC and VCC without any statistical correlation between them. The collisional contribution to the density-matrix can be written as [16, 19]

$$\begin{aligned}\left(\frac{\partial\rho'}{\partial t}\right)_{\text{collision}} &= -\gamma_{P_{mn}}(v)(1-\delta_{mn})\rho'_{mn} - \alpha_{mn}(v)\rho'_{mn} \\ &\quad + \int \mathrm{d}v'\, W_{mn}(v'\to v)\rho'_{mn}(v',t),\end{aligned} \tag{2}$$

where, the rate of PDC, $\gamma_{P_{mn}}(v)$ has no contribution to the diagonal term of ρ'. The term, $\alpha_{mn}(v)$ indicates the kinetic collision rate at which active atoms leave velocity subclass, v, whereas the last term of Eq. (2) is the rate of return to the subclass, v (see Ref. [16]). By considering slow variation of $\gamma_{P_{mn}}(v)$ and $\alpha_{mn}(v)$ with v, we can neglect the velocity dependence of these quantities. We explain the collision phenomena by employing strong-collision model [20]. The collision kernel is then written as $W_{mn}(v'\to v) = \alpha_{mn}f_{\text{MB}}(v)$, where $f_{\text{MB}}(v)$ is the Maxwell-Boltzmann velocity distribution given by $f_{\text{MB}}(v) = \sqrt{M_{\text{A}}/(2\pi k_{\text{B}}T)}\exp\{-M_{\text{A}}v^2/(2k_{\text{B}}T)\}$; M_{A} is the atomic mass, k_{B} is the Boltzmann constant and T is the absolute temperature. The strong velocity dependence of excitation rates is discarded [15]. So, we can define $\Lambda_m(v) = \Lambda_m f_{\text{MB}}(v)$. We should mention here that our present work is restricted to the collisional regime where PDC dominates over VCC. In order to remove rapid time dependence of off-diagonal elements of the density-matrix, ρ', we use the transformations, $\rho'_{mm} = \rho_{mm}$, $\rho'_{jk} = \rho_{jk}$ for $j \neq k$ and $\rho'_{1j} = \mathrm{e}^{-\mathrm{i}\omega t}[\rho'^{+}_{1j}\mathrm{e}^{\mathrm{i}k_z z} + \rho'^{-}_{1j}\mathrm{e}^{-\mathrm{i}k_z z}]$, $k = 2,3$, where positive and negative signs are taken to designate the propagation of the fields in the z-direction and in the opposite direction, respectively. Now, the components of the density-matrix elements of Eq. (1) can be represented by taking

the rotating-wave approxation (RWA) [21] as follows,

$$\frac{\partial \rho_{11}}{\partial t} = \Lambda_1 f_{\rm MB}(v) - \big(\gamma_1 + \alpha_{11}\big)\rho_{11} + \frac{1}{2}\sum_{j=2,3} R_{1j}{\rm Re}\{\rho_{1j}^{+} - \rho_{1j}^{-}\} + \alpha_{11} f_{\rm MB}(v)\int \rho_{11}(v',t)\,{\rm d}v', \tag{3}$$

$$\frac{\partial \rho_{jj}}{\partial t} = \Lambda_j f_{\rm MB}(v) - \big(\gamma_j + \alpha_{jj}\big)\rho_{jj} - \frac{1}{2}R_{1j}{\rm Re}\{\rho_{1j}^{+} - \rho_{1j}^{-}\} + \alpha_{jj} f_{\rm MB}(v)\int \rho_{jj}(v',t)\,{\rm d}v', \tag{4}$$

$$\frac{\partial \rho_{1j}^{\pm}}{\partial t} = \pm\frac{1}{4}R_{1j}(\rho_{jj} - \rho_{11}) \pm \frac{1}{4}\big(R_{1k}\rho_{kj}\big)_{k\neq j} - \big[\Gamma_{1j} + {\rm i}(\Delta_{1j} \pm k_z v)\big]\rho_{1j}^{\pm}\,, \tag{5}$$

$$\left(\frac{\partial \rho_{jk}}{\partial t}\right)_{j\neq k} = -\frac{1}{4}R_{1j}(\rho_{1k}^{+} - \rho_{1k}^{-}) - \frac{1}{4}R_{1k}(\rho_{j1}^{+} - \rho_{j1}^{-}) - \big[\gamma_{jk} + \gamma_{P_{jk}} + {\rm i}\omega_{jk}\big]\rho_{jk}\,, \tag{6}$$

where $\Gamma_{1j} = \gamma_{1j} + \gamma_{P_{1j}} + \alpha_{1j}$. If the angle ϕ is a measure of Raman coherence between levels $|2\rangle$ and $|3\rangle$ [22], then in a steady state we can assume from Eq. (6) $\rho_{23} = \sigma(v){\rm e}^{{\rm i}\phi}/[(\gamma_{23} + \gamma_{P_{23}})^2 + \omega_{23}^2]$, where the amplitude factor, $\sigma(v)$ denotes basically the strength of coherent coupling, and the phase angle ϕ can be taken as the degree of coherence. In the present formulation, strong velocity correlation of $\sigma(v)$ is omitted to write $\sigma(v) = \sigma f_{\rm MB}(v)$.

By following the rate equation (5), in steady state, the expression of ρ_{1j} can be written as follows,

$$\rho_{1j}^{\pm} = \pm\frac{R_{1j}(\rho_{jj} - \rho_{11}) + \big(R_{1k}\big)_{k\neq j}\sigma'(v){\rm e}^{-{\rm i}\phi}}{4\big[\Gamma_{1j} + {\rm i}(\Delta_{1j} \pm k_z v)\big]}\,, \tag{7}$$

where $\sigma'(v) = \sigma f_{\rm MB}(v)/[(\gamma_{23} + \gamma_{P_{23}})^2 + \omega_{23}^2]$. No perturbative approach has been undertaken to solve the coupled Eqs. (3) – (5) in steady state to obtain the population terms, ρ_{11} and ρ_{jj} in Eq. (7). Rearranging the expressions of $\rho_{1j}^{\pm}$ for real and imaginary parts, we have ${\rm Re}\{\rho_{1j}^{+} - \rho_{1j}^{-}\}$ of the following forms

$${\rm Re}\{\rho_{12}^{+} - \rho_{12}^{-}\} = g_1(\rho_{22} - \rho_{11}) + g_2\sigma'(v)\,, \tag{8}$$

where

$$g_1 = \frac{1}{4}R_{12}L_{12}, \quad g_2 = \frac{1}{4}R_{13}\big(\Gamma_{12}L_{12}\cos\phi - L'_{12}\sin\phi\big)\,,$$

$$L_{12} = \frac{\Gamma_{12}}{\Gamma_{12}^2 + (\Delta_{12} + k_z v)^2} + \frac{\Gamma_{12}}{\Gamma_{12}^2 + (\Delta_{12} - k_z v)^2}\,,$$
$$L'_{12} = \frac{\Delta_{12} + k_z v}{\Gamma_{12}^2 + (\Delta_{12} + k_z v)^2} + \frac{\Delta_{12} - k_z v}{\Gamma_{12}^2 + (\Delta_{12} - k_z v)^2}\,,$$

and

$$\mathrm{Re}\{\rho_{13}^{+} - \rho_{13}^{-}\} = h_1(\rho_{33} - \rho_{11}) + h_2\sigma'(v)\,, \tag{9}$$

where

$$h_1 = \frac{1}{4}R_{13}L_{13}, \quad h_2 = \frac{1}{4}R_{12}\big(\Gamma_{13}L_{13}\cos\phi - L'_{13}\sin\phi\big)\,,$$
$$L_{13} = \frac{\Gamma_{13}}{\Gamma_{13}^2 + (\Delta_{13} + k_z v)^2} + \frac{\Gamma_{13}}{\Gamma_{13}^2 + (\Delta_{13} - k_z v)^2}\,,$$
$$L'_{13} = \frac{\Delta_{13} + k_z v}{\Gamma_{13}^2 + (\Delta_{13} + k_z v)^2} + \frac{\Delta_{13} - k_z v}{\Gamma_{13}^2 + (\Delta_{13} - k_z v)^2}\,.$$

Here L_{1j} and L'_{1j} reflect the absorptive and dispersive contributions of the respective transitions into $\mathrm{Im}\{\chi_+\}$. As far as the statistical independence between velocity subclasses is concerned, in steady state, we have the choice to introduce $\int \rho_{mm}(v')\,\mathrm{d}v' = \int \rho_{mm}(v'')\,\mathrm{d}v'' = \int \rho_{mm}(v)\,\mathrm{d}v = f_m$ for diagonal elements of the density matrix Eqs. (3) and (4). Here f_m implies the constant contribution of the integrals for different velocity subclasses represented by v', v'' and v. By inserting $\mathrm{Re}\{\rho_{1j}^{+} - \rho_{1j}^{-}\}$ and f_m in the steady state equations of diagonal elements of the density matrix Eqs. (3),(4), we solve the simultaneous equations corresponding to ρ_{mm} to obtain

$$\rho_{11} = (X_1 + X_2)f_{\mathrm{MB}}(v)\,, \tag{10}$$
$$\rho_{22} = (-b_1 + b_2(X_1 + X_2) + b_3 f_2)f_{\mathrm{MB}}(v)\,, \tag{11}$$
$$\rho_{33} = (-c_1 + c_2(X_1 + X_2) + c_3 f_3)f_{\mathrm{MB}}(v)\,. \tag{12}$$

The terms, b_m, c_m, X_m and f_m, pertaining to Eqs. (10) – (12) are given in Appendix A. The complex polarization induced in the atom can be written for optical coherence term, ρ_{1j}^{+},

$$P_+(z,t) = N\sum_{j=2,3}\mu_{1j}\left[\int \rho_{1j}^{+}(\Delta_{1j}, v)\,\mathrm{d}v\,\mathrm{e}^{\mathrm{i}(k_z z - \omega t)} + \mathrm{c.c.}\right], \tag{13}$$

where N is the density of atomic vapours. We can define the susceptibility (χ_+) by setting the polarization [21]

$$P_+(z,t) = -\epsilon\sum_{j=2,3}\left[\mathrm{i}\chi_{1j}^{+}\mathrm{e}^{\mathrm{i}(k_z z - \omega t)} - \mathrm{i}\big(\chi_{1j}^{+}\big)^{*}\mathrm{e}^{-\mathrm{i}(k_z z - \omega t)}\right]. \tag{14}$$

By assuming $\mu_{12} = \mu_{13} = \mu$, we can find the absorption coefficient from Eqs. (13) and (14),

$$\mathrm{Im}\{\chi_+\} = \frac{N\mu}{\epsilon} \sum_{j=2,3} \int \mathrm{Re}\{\rho_{1j}^{+}(\Delta_{1j}, v)\}\, \mathrm{d}v\,. \tag{15}$$

The resonant absorption in the medium can be explained either by $\mathrm{Im}\{\chi_+\}$, or by $\mathrm{Im}\{\chi_-\}$ corresponding to ρ_{1j}^{-} $(j = 2, 3)$ in the present work. If the absorbtion is probed along the $(+)$ direction, then the $(-)$ direction implies the propagation of the pump field through the medium.

3. Results and discussion

We have computed numerically the saturated absorption profile for various physical conditions by introducing the detuning parameter, $\Delta = \Delta_{1j} \pm (1/2)\omega_{23}$ ($(+)$ and $(-)$ signs correspond to $j = 2$ and $j = 3$, respectively). The Rabi frequencies corresponding to different resonances are assumed to be the same. Figure l demonstrates the saturated absorption line shapes for different values of Rabi frequency and upper level separation ω_{23} at different Doppler broadened backgrounds when the system is guided by the spontaneous relaxation processes only. If we compare the

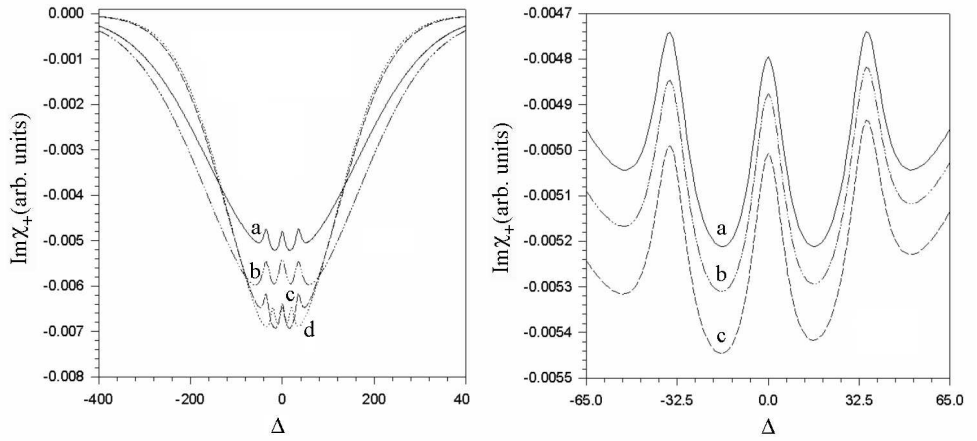

Fig. 1 (left). Saturated absorption line shapes for fixed values of $\gamma_1 = \gamma_2 = \gamma_3 = 5$, $\Lambda_1 = 2$, $\Lambda_2 = \Lambda_3 = 1$, $\gamma_{P_{12}} = \gamma_{P_{13}} = \gamma_{P_{23}} = 0$, $\alpha_{11} = \alpha_{22} = \alpha_{33} = 0$, $\sigma = 0.01$ *and* $\phi = \pi/4$. *Values of other parameters are,* $W_D = 180$, $R_{12} = R_{13} = 10$ *and* $\omega_{23} = 70$ *for curve a,* $W_D = 180$, $R_{12} = R_{13} = 20$ *and* $\omega_{23} = 70$ *for curve b,* $W_D = 130$, $R_{12} = R_{13} = 10$ *and* $\omega_{23} = 70$ *for curve c and* $W_D = 130$, $R_{12} = R_{13} = 10$ *and* $\omega_{23} = 40$ *for curve d. All rates are taken in the units of* γ_{23} *(see text).*

Fig. 2. Saturated absorption line shapes for various σ *and* ϕ *(curve a for* $\sigma = 0.01$, $\phi = \pi/4$, *curve b for* $\sigma = 1$, $\phi = \pi/4$ *and curve c for* $\sigma = 1$, $\phi = \pi/3$*). Other parameters are the same as those of curve a of Fig. l.*

curves a and b, we see that the increase of amplitude of the external field enhances the saturation process. This results in more distinct and symmetric Lamb dips and crossover dip in curve b than that observed in curve a. If the difference between the value of the inhomogeneous broadening parameter and ω_{23} is reduced, the traces of Lamb dips become less prominent in comparison to the crossover peak (curve c) within Doppler limited regime. The response of the Lamb dip and crossover resonances into the absorption profile would have been symmetric (curve d) for smaller values of ω_{23}. If the coherent coupling between the two excitation paths is made stronger by increasing the value of the amplitude factor related to the coherence term, ρ_{23}, the saturation depth will be increased as exhibited by curves a and b in Fig. 2. In comparison to the curve a, the curve b shows a small asymmetry induced in the wings of the Lamb dip profiles within the Doppler-broadened line shape. At larger value of the degree of coherence (the phase angle, ϕ), induced asymmetry will be enhanced as shown by curve c. This fact may be one of the reasons for the asymmetries observed in the distribution of the Lamb dips and crossover dips for ^{87}Rb D_2-transition ($F_g = 2$ to $F_e = 1, 2, 3$) in Ref. [23]. In order to obtain the collision-induced line shapes, the Raman coherence parameters are taken to be the same as those of curve a of Fig. 2. Figure 3 depicts the collision-induced behaviour of the saturated profiles for small contribution of VCC compared to PDC as expected in our collisional regime mentioned earlier. With increasing values of

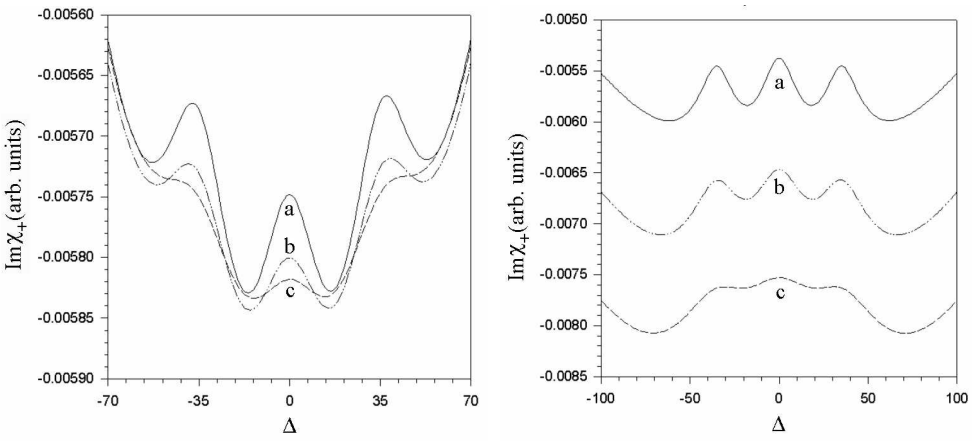

Fig. 3 (left). Saturated absorption line shapes for various $\gamma_{P_{1j}}$ and $\gamma_{P_{23}}$, and fixed values of α_{jj} ($\alpha_{11} = \alpha_{22} = \alpha_{33} = 0.5$). Curve a stands for $\gamma_{P_{12}} = \gamma_{P_{13}} = 10$, $\gamma_{P_{23}} = 5$, curve b for $\gamma_{P_{12}} = \gamma_{P_{13}} = \gamma_{P_{23}} = 13$ and curve c for $\gamma_{P_{12}} = \gamma_{P_{13}} = 17$, $\gamma_{P_{23}} = 15$. Other parameters are the same as those of curve a of Fig. 1.

Fig. 4. Saturated absorption line shapes at higher values of Rabi frequencies ($R_{12} = R_{13} = 25$) for various $\gamma_{P_{1j}}$ and $\gamma_{P_{23}}$, and for smaller values of α_{jj}. Curve a stands for $\gamma_{P_{12}} = \gamma_{P_{13}} = \gamma_{P_{23}} = 0$, $\alpha_{11} = \alpha_{22} = \alpha_{33} = 0$, curve b for $\gamma_{P_{12}} = \gamma_{P_{13}} = \gamma_{P_{23}} = 4$, $\alpha_{11} = \alpha_{22} = 0.02$, $\alpha_{33} = 0.07$ and curve c for $\gamma_{P_{12}} = \gamma_{P_{13}} = \gamma_{P_{23}} = 12$, $\alpha_{11} = \alpha_{22} = 0.01$, $\alpha_{33} = 0.05$. Other parameters remain fixed as that in Fig. 3.

phase-dephasing collision-parameters, nonlinear response of the absorption profile goes on decreasing as predicted by curves a, b and c in Fig. 3 for an optimum choice of collision kernels ($\alpha_{11} = \alpha_{22} = \alpha_{33}$). Figure 4 shows the saturated line shapes at collision-free (curve a) and collision-induced conditions (curves b and c) for larger value of Rabi frequency than that in Fig. 3. The resonant and nonresonant peaks in Fig. 4 become suppressed at relatively lower values of phase-dephasing collision-parameters than used in Fig. 3, for the same value of the Doppler broadening, when the contribution of saturation broadening is sufficiently large. If the contribution of PDC is kept unchanged, the asymmetry can be imposed to the Doppler-limited absorption profile for different sets of collision kernels, as shown by curves a, b and c in Fig. 5. At high value of Rabi frequency, asymmetry is found to be significant for small contribution of VCC. A sufficient increment of the values of the phase-dephasing collision parameters can cause the saturated behaviour to be washed out within the Doppler-broadened absorption as indicated by curve d in Fig. 5.

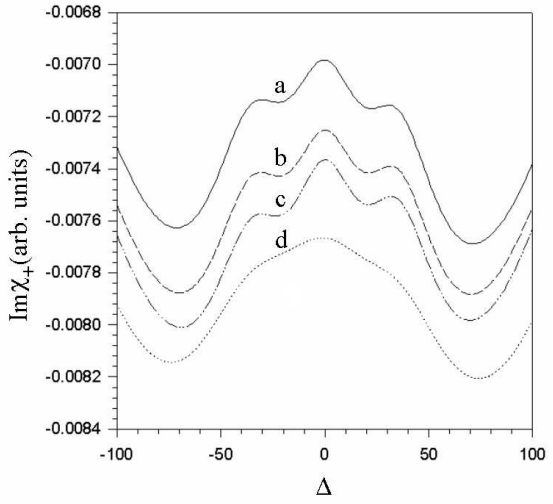

Fig. 5. Saturated absorption line shapes for various $\gamma_{P_{1j}}$, $\gamma_{P_{23}}$ and α_{jj}. Curve a stands for $\gamma_{P_{12}} = \gamma_{P_{13}} = \gamma_{P_{23}} = 10$, $\alpha_{11} = 0.05$, $\alpha_{22} = 0.02$, $\alpha_{33} = 0.8$, curve b for $\gamma_{P_{12}} = \gamma_{P_{13}} = \gamma_{P_{23}} = 10$, $\alpha_{11} = \alpha_{22} = 0.17$, $\alpha_{33} = 0.4$, curve c for $\gamma_{P_{12}} = \gamma_{P_{13}} = \gamma_{P_{23}} = 10$, $\alpha_{11} = \alpha_{22} = \alpha_{33} = 0.4$ and curve d for $\gamma_{P_{12}} = \gamma_{P_{13}} = \gamma_{P_{23}} = 20$, $\alpha_{11} = 0.05$, $\alpha_{22} = 0.02$, $\alpha_{33} = 0.8$. Other parameters remain fixed as that in Fig. 4.

4. Conclusion

In this work we have presented the Doppler-broadened absorption line shape for coherently-coupled closely-spaced transitions in the presence of a standing wave field. In order to obtain the absorption coefficient, the density-matrix equations have been solved in the steady state without applying any perturbation mathod. In the derivation of absorptive line shape, we have introduced two physical entities

σ and ϕ related to the coherent coupling term, ρ_{23}. For the simulation of the line shape from experimentally observed data, σ and ϕ can be taken as adjustable parameters along with other parameters required for the least-squares fitting process. In our formulation, the computed line profiles show the relative influence of the collision effects, PDC and VCC on the saturation behaviour of Doppler-broadened absorption at various physical conditions. The appearence of the Lamb dips and the crossover resonance dip can be washed out for a sufficient contribution of PDC in the presence of VCC at a high value of Rabi frequency. The asymmetry may arise in the wings of the saturated-line shapes within the Doppler limit due to the small contribution of VCC. We have checked that there is no shifting of positions of Lamb dip resonances within the variation of the Rabi frequency. This fact could have been observed if the value of the Rabi frequency would be very much smaller compared to the separation of the upper levels and the tranverse relaxation rates [17].

Appendix

$$X_1 = -\frac{a_1 + a_2 b_1 + a_3 c_1}{1 - a_2 b_2 - a_3 c_2}\,, \qquad X_2 = \frac{a_4 f_1 + a_2 b_3 f_2 + a_3 c_3 f_3}{1 - a_2 b_2 - a_3 c_2}\,,$$

$$f_1 = \frac{a_1 b_4 c_4 - a_2 b_1 c_4 - a_3 b_4 c_1}{Z}\,, \qquad f_2 = \frac{a_5 b_1 c_4 - a_1 b_2 c_4 - a_3 (b_2 c_1 - c_2 b_1)}{Z}\,,$$

$$f_3 = \frac{a_5 b_4 c_1 - a_1 b_4 c_2 - a_2 (b_2 c_1 - c_2 b_1)}{Z}\,, \qquad Z = a_5 b_4 c_4 - a_2 b_2 c_4 - a_3 b_4 c_2\,,$$

$$a_1 = -\frac{2\Lambda_1 + R_{12} g_2 \sigma_0 + R_{13} h_2 \sigma_0}{2a}\,, \qquad a_2 = \frac{R_{12} g_1}{2a}\,,$$

$$a_3 = \frac{R_{13} h_1}{2a}\,, \qquad a_4 = \frac{\alpha_{11}}{a}\,, \qquad a_5 = a_4 - 1\,,$$

$$\sigma_0 = \frac{\sigma}{(\gamma_{23} + \gamma_{P_{23}})^2 + \omega_{23}^2}\,, \qquad a = \gamma_1 + \alpha_{11} + \frac{R_{12} g_1}{2} + \frac{R_{13} h_1}{2}\,,$$

$$b_1 = -\frac{2\Lambda_2 - R_{12} g_2 \sigma_0}{2b}\,, \qquad b_2 = \frac{R_{12} g_1}{2b}\,,$$

$$b_3 = \frac{\alpha_{22}}{b}\,, \qquad b_4 = b_3 - 1\,, \qquad b = \gamma_2 + \alpha_{22} + \frac{R_{12} g_1}{2}\,,$$

$$c_1 = -\frac{2\Lambda_3 - R_{13} h_2 \sigma_0}{2c}\,, \qquad c_2 = \frac{R_{13} h_1}{2c}\,,$$

$$c_3 = \frac{\alpha_{33}}{c}\,, \qquad c_4 = c_3 - 1\,, \qquad c = \gamma_3 + \alpha_{33} + \frac{R_{13} h_1}{2}\,.$$

References

[1] W. R. Bennet, Phys. Rev. **126** (1962) 580.

[2] *Persistent Spectral Hole-Burning: Science and Applications*, ed. W. E. Moerner, *Topics in Current Physics*, Vol. 44, Springer, Berlin (1988).

[3] W. E. Lamb, Phys. Rev. **134A** (1964) 1429.

[4] S. Haroche and F. Hartmann, Phys. Rev. A **6** (1972) 1280.

[5] H. R. Schlossberg and A. Javan, Phys. Rev. **150** (1966) 267.

[6] T. W. Hansch, N. H. Nayfeh, S. A. Lee, S. M. Curry and I. S. Shahin, Phys. Rev. Lett. **32** (1974) 1336.

[7] J. L. Hall and C. Borde, Phys. Rev. Lett. **30** (1973) 1101.

[8] S. S. Kim, S. E. Park, H. S. Lee, C. H. Oh, J. D. Park and H. Cho, Jpn. J. Appl. Phys. **32** (1993) 3291.

[9] J. Ye, S. Swartz, P. Jungner and J. L. Hall, Opt. Lett. **21** (1996) 1280.

[10] A. C. Park, H. S. Lee, T. Y. Kwon and H. Cho, Opt. Commun. **92** (2001) 49.

[11] T. Loftus, J. R. Bochinski and T. W. Mossberg, Phys. Rev. A **63** (2001) 023402.

[12] U. Tanaka and T. Yabuzaki, Jpn. J. Appl. Phys. **33** (1994) 1614.

[13] K. B. McAdam, A. Steinbach and C. E. Wieman, Am. J. Phys. **60** (1992) 1098.

[14] T. W. Hansch, I. S. Shahin and A. L. Schawlow, Phys. Rev. Lett. **27** (1971) 707.

[15] A. Agarwal and R. Ghosh, Phys. Rev. A **47** (1993) 1407.

[16] S. Singh and G. S. Agarwal, Phys. Rev. A **42** (1990) 3070.

[17] S. Mandal and P. N. Ghosh, Phys. Rev. A **45** (1992) 4990.

[18] D. Bhattacharyya, B. K. Dutta, B. Ray and P. N. Ghosh, Chem. Phys. Lett. **389** (2004) 113.

[19] P. R. Berman, in *New Trends in Atomic Physics*, eds. G. Grynberg and R. Stora, North-Holland, Amsterdam (1984).

[20] S. G. Rautian and I. I. Sobelman, Sov. Phys. Usp. **9** (701) 1966.

[21] S. Stenholm, *Foundations of Laser Spectroscopy*, Wiley, New York (1983).

[22] M. O. Scully, Phys. Rev. Lett. **67** (1991) 1855.

[23] D. Bhattacharyya, B. K. Dutta, B. Ray and P. N. Ghosh, Fizika A (Zagreb) **12** (2003) 171.

PROUČAVANJE UČINAKA BRZINSKI-OVISNIH SUDARA NA LAMBOVU UDUBINU I PRIJELAZNE REZONANCIJE U SUSTAVU S TRI STANJA

Raspravljamo učinke otklanjanja faze i sudara s promjenom brzine na oblike linija zasićenih apsorpcijom za otvoren V-sustav, primjenom poluklasičnog formalizma matrice gustoće. Primijetili smo da tragovi Lambovih udubina i prijelaznih rezonancija unutar linija proširenih Dopplerovih učinkom mogu nestati pod djelovanjem snažnog zasićujećeg polja uz dovoljan doprinos učinka sudarnog otklanjanja faza. U ramenima zasićenih linija može se postići nesimetrija za male doprinose sudarne jezgre.